

General Disclaimer

One or more of the Following Statements may affect this Document

- This document has been reproduced from the best copy furnished by the organizational source. It is being released in the interest of making available as much information as possible.
- This document may contain data, which exceeds the sheet parameters. It was furnished in this condition by the organizational source and is the best copy available.
- This document may contain tone-on-tone or color graphs, charts and/or pictures, which have been reproduced in black and white.
- This document is paginated as submitted by the original source.
- Portions of this document are not fully legible due to the historical nature of some of the material. However, it is the best reproduction available from the original submission.

CR-151345

FINAL REPORT

DEFINITION AND FABRICATION OF AN AIRBORNE SCATTEROMETER RADAR SIGNAL PROCESSOR

(NASA-CR-151345) DEFINITION AND FABRICATION
OF AN AIRBORNE SCATTEROMETER RADAR SIGNAL
PROCESSOR Final Report (Texas A&M Univ.)
60 p HC A04/MF A01

CSCL 17I

N77-23291

Unclas

G3/32 26088

December 1976



National Aeronautics and Space Administration
Contract NAS9-14493



TEXAS A&M UNIVERSITY
REMOTE SENSING CENTER
COLLEGE STATION, TEXAS



TABLE OF CONTENTS

	<u>Page</u>
TABLE OF CONTENTS	i
<u>ABSTRACT</u>	ii
<u>INTRODUCTION</u>	1
<u>PROCESSOR SPECIFICATIONS</u>	3
<u>SYSTEM OPERATION</u>	7
<u>The Radar Equation</u>	7
<u>Radar Scatterometers</u>	10
<u>Spectrum Folding and 'Sign-Sensing'</u>	13
<u>Spectrum Sampling and Cell Definition</u>	15
<u>Coefficient Calculation</u>	17
<u>Alignment</u>	21
<u>Processing Requirements</u>	21
<u>Functional Organization</u>	22
<u>HARDWARE</u>	24
<u>The Analog Subsystem</u>	24
<u>The Digital Subsystem</u>	30
<u>SOFTWARE</u>	34
<u>Modes</u>	34
<u>Arithmetic</u>	39
<u>Area Calculation</u>	44
<u>Coefficient Alignment Procedure</u>	46
<u>CONCLUSIONS AND RECOMMENDATIONS</u>	53
<u>REFERENCES</u>	56

ABSTRACT

A real-time processor for NASA 13.3 single-polarized scatterometer data has been developed at the Remote Sensing Center, Texas A&M University. This processor is a hardware/software system which incorporates a microprocessor design and software for the calculation of normalized radar cross section in real time. Interface is provided to decommutate the NASA ADAS data stream for aircraft parameters used in processing and to provide output in the form of strip chart and pcm compatible data recording. The unit has been delivered to NASA/JSC.

AN AIRBORNE RADAR SCATTEROMETER SIGNAL PROCESSING SYSTEM

INTRODUCTION

The Remote Sensing Center at Texas A&M University has developed for the National Aeronautics and Space Administration (NASA) a real-time signal processor to be used in conjunction with the NASA/Johnson Space Center (JSC) 13.3 GHz single polarized radar scatterometer system. It was the object of this development effort to provide a processing capability to speed the evaluation of scatterometer data in earth resources investigations and provide data in a form that shortens the processing time required to produce a final product with respect to existing data reduction procedures.

The effort was conducted in three phases. Phase I was a definition study and provided for the specification of the hardware design. Phase II provided for the fabrication of hardware and the development of test procedures and documentation. Phase III provided for the checkout and testing of the signal processor and for the delivery of the processor unit to NASA/JSC.

This report constitutes the final report for the project. In this report the general requirements for the processing of scatterometer data are outlined

and the general theory of operation of the developed processor is developed. This report, together with the Processor Operation and Maintenance document, constitutes the bulk of the project documentation.

PROCESSOR SPECIFICATIONS

The Real-Time Airborne Scatterometer Signal Processor (RASP) is a developmental extension of previous work done in real-time processing of scatterometer signals at Texas A&M University (TAMU). This work was done for the Naval Surface Weapons Center (NSWC) (formerly Naval Ordnance Laboratory) and resulted in hardware designs and implementation of analog processing systems for the real-time classification of sea ice types from 13.3 GHz scatterometer measurements [1]. This previous development and subsequent advances in large scale integration in solid state electronics, and microprocessor development established the feasibility of the design and construction of a real-time processor unit using combined analog and digital (hybrid) signal processing techniques.

The project to design and construct the RASP unit was undertaken to bridge the gap between previous processor development and the availability of a fully developed processor system which could provide for in-flight evaluation of the techniques of real-time signal processing. This unit could also provide a signal reduction capability for the 13.3 GHz scatterometer system so that processed results from data missions would be available for prompt evaluation of mission effectiveness in acquiring suitable scatterometer data. This evaluation of processed data

would also identify flight segments for which more precise data product could be obtained from other processing capabilities such as the existing NASA scatterometer data reduction software or the software package under development at Texas A&M.

The RASP processor was designed and constructed as a single chassis unit using printed circuit wire wrap boards, large scale integrated circuits and hybrid electronics, see Figure 1. The design centered around an Intel 8080 microprocessor system. The RASP unit uses the latest technology available on a production basis and incorporates system designs which are advanced state-of-the-art in scatterometer signal processing.

The RASP processor was implemented to interface with several aircraft data systems. Aircraft flight parameters are input in either ADAS or NERDAS data formats from NASA flight systems and processor data output is available for strip chart recording. The output data are also provided by the processor in a Bi-phase Level (BIØ-L) pcm compatible format for recording. Documentation of these data reduction results provides a computer compatible format for further analysis and data tabulation.

The principal data output product from the RASP processor is the tabulation of normalized radar cross section or scattering coefficient as a function of incident

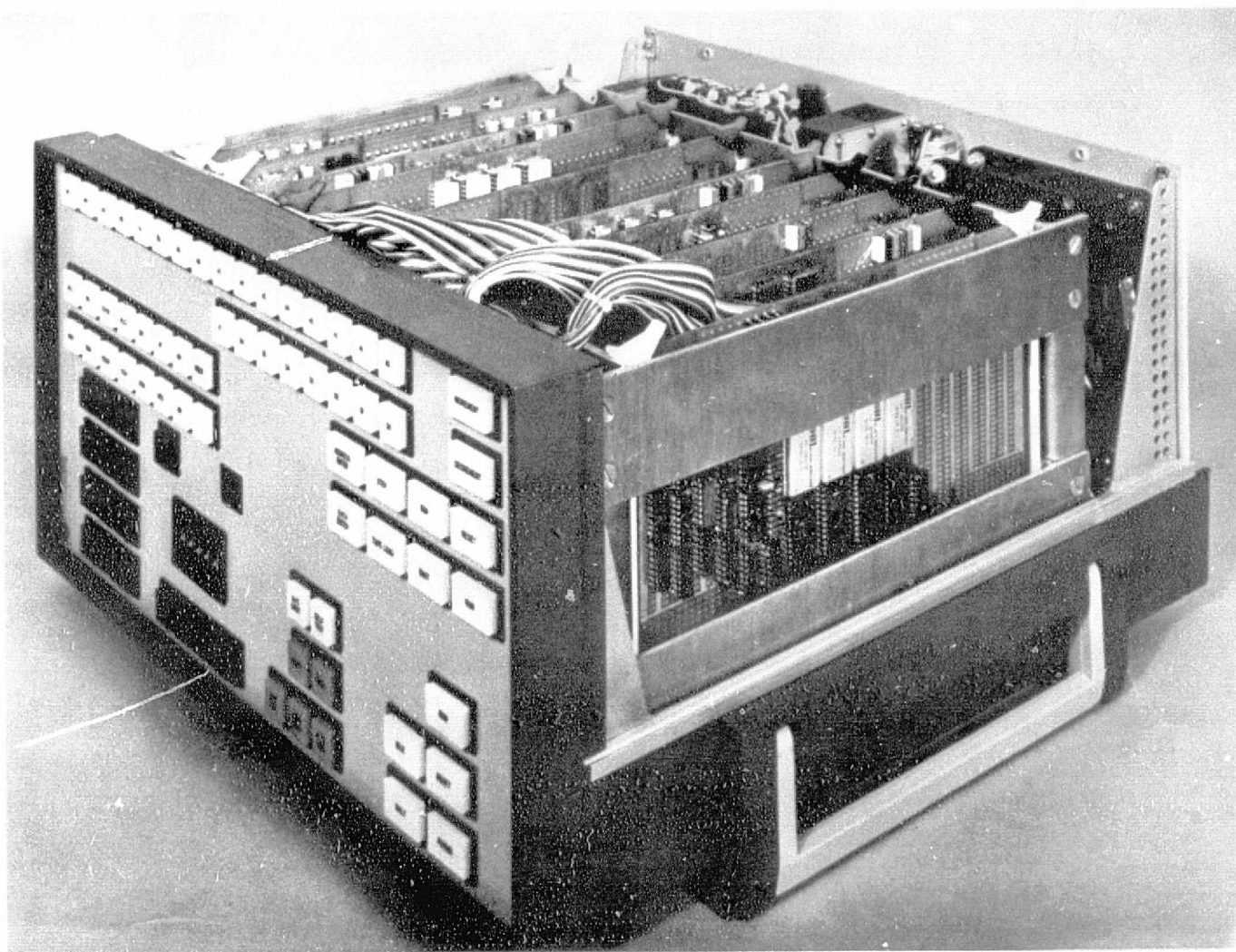


Figure 1. Real-Time Airborne Scatterometer
Signal Processor (RASP)

angle which is aligned for an illuminated target cell. These coefficients are calculated dynamically using instantaneous values of the aircraft flight parameters and radar signals. This is an improvement on previous processing techniques which primarily utilize average aircraft flight parameters. The concept of real-time processing of scatterometer data also presents a novel approach to time-of-flight evaluation of mission success and timely consideration of processed data results.

SYSTEM OPERATION

The RASP system is designed to interface with the NASA 13.3 GHz single polarized scatterometer system. An understanding of this instrument and its signal outputs is essential to the design of the processor system. The NASA scatterometer is an active microwave sensor, a radar, which illuminates a target area with microwave energy and receives the return which is scattered from the target. Subsequently, the return signals are modified and recorded for signal reduction and processing.

The Radar Equation

The radar equation is used to describe the viewing of a target by a radar system. The following development of the radar equation follows that of Moore in [2, equations 9-66 through 9-69, p.419].

Consider the geometry of a radar remote sensor as illustrated in Figure 2. The power density at the target is that from an antenna of transmitter gain G_t radiating a power P_t upon a target at range R , thus,

$$\text{Power density at target} = \frac{P_t G_t}{4\pi R^2}$$

The power received at the receiving antenna is the power density of the target backscatter across the effective

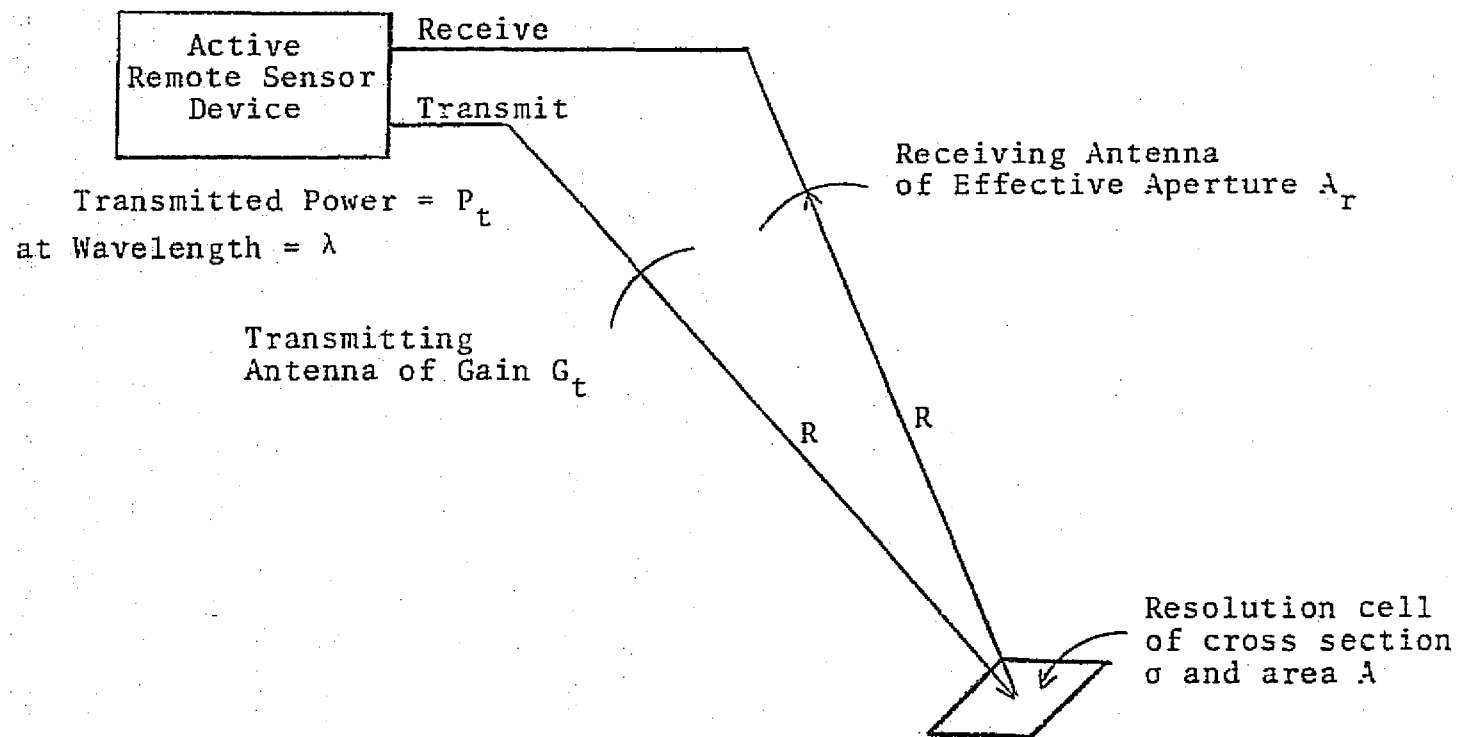


Figure 2. Active Remote Sensor Configuration

aperture of the receiving antenna, that is,

$$\text{Power received} = P_r = \frac{P_t G_t}{4\pi R^2} \cdot \sigma \cdot \frac{1}{4\pi R^2} A_r$$

where σ is the effective backscatter area or cross section of the target, and A_r is the effective receiver aperture.

If the radar system employs a duplexed antenna, i.e., if the receiver and transmitter utilize the same antenna, or if antennas of equal parameters are used for receiver and transmitter, then the relationship

$$G_t = G_r = G = \frac{4\pi A_r}{\lambda^2}$$

reduces the equation for received power to give one form of the radar equation:

$$P_r = \frac{P_t G^2 \lambda^2 \sigma}{(4\pi)^3 R^4}$$

The quantity in the radar equation of most interest to investigators is the radar cross section σ , since it is the only parameter relating information about the target. The cross section is generally expressed as an average over the cell area, A , and has been demonstrated [3, 4] to be a function of several parameters. They are,

$$\sigma^0 = \sigma/A = f(F, P, \theta, \phi, S, \epsilon)$$

where

σ^0 = normalized target cross section

F = frequency of incident energy

P = polarization of incident energy

θ = angle of incidence

ϕ = target aspect angle

S = surface roughness factor, and

ϵ = target complex dielectric constant

Remote sensing applications rely on the cross section's dependence on the latter two factors, the surface roughness and dielectric constant of the target cell. These two factors are indicative of important surface parameters. For example, soil moisture content affects the dielectric constant [5], and wind speed over large bodies of water has been related to the surface roughness [4, 6, 7].

Radar Scatterometers

An important class of radar systems is the continuous wave (CW) scatterometer. A CW scatterometer irradiates the target with a continuous beam of energy and receives the return energy at a separate antenna. This return power may be compared to the transmitted power to determine the scattering cross section. The NASA 13.3 GHz scatterometer system, for which the data

processor was developed, is one of this class of scatterometers. This system illuminates the area beneath the aircraft with an antenna beam plus and minus 60° from the nadir along track and 3° wide across track. Figure 3 illustrates the area illuminated by the NASA system.

As the name implies, CW Doppler systems utilize the Doppler effect; that is, the change in frequency of energy emitted from a source because of a velocity difference between the source and the receiver. For an airborne CW Doppler system moving horizontally over the earth, the Doppler effect causes a return spectrum of frequencies from the illuminated area, with positive Doppler shifts from the fore targets (approaching), and negative shifts from the aft targets (receding).

The amount of Doppler frequency shift, f_d , introduced into the radar return from a particular point on the ground is related to the incident energy frequency, f_i , by

$$f_d = \frac{2v_r f_i}{c}$$

where

v_r = relative velocity of target toward the receiver,
and

c = propagation velocity, 3×10^8 m/sec.

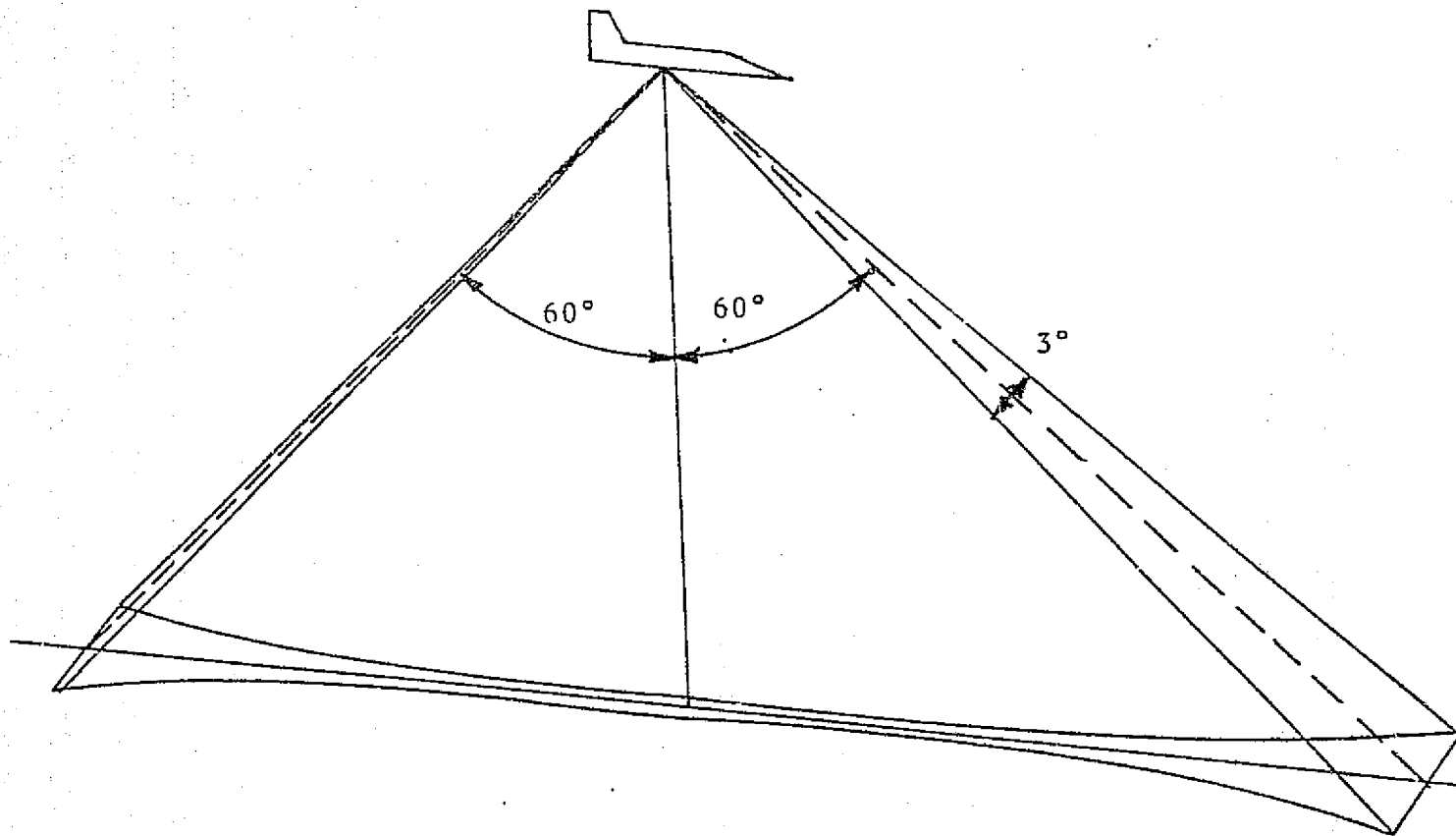


Figure 3. The NASA System Fan-beam Antenna Pattern

Since the relative velocity can be positive or negative, the return power is usually distributed in an asymmetric spectrum centered around the transmitted frequency. Thus, with a CW Doppler system, the return from a particular angle of incidence has a unique corresponding frequency in the return spectrum.

Spectrum Folding and 'Sign-Sensing'

The processing of the data is difficult to achieve at the high transmitter frequency; therefore, the return signal is heterodyned at the radar receiver with a portion of the transmitter energy to produce a baseband signal. Unfortunately, this causes a "folding" of the fore and aft Doppler frequencies about zero Hertz in the frequency spectrum. In the NASA system, two baseband signals, termed the sine and cosine channels, are provided by splitting the received signal into quadrature signals before mixing. Figure 4 illustrates the nature of these two signals. Additionally, a signal proportional to the transmitter power is inserted into the cosine channel. Recovery of the fore and aft Doppler spectra (sign-sensing) and of the calibration signal is an essential step in the reduction of the 13.3 GHz scatterometer signals.

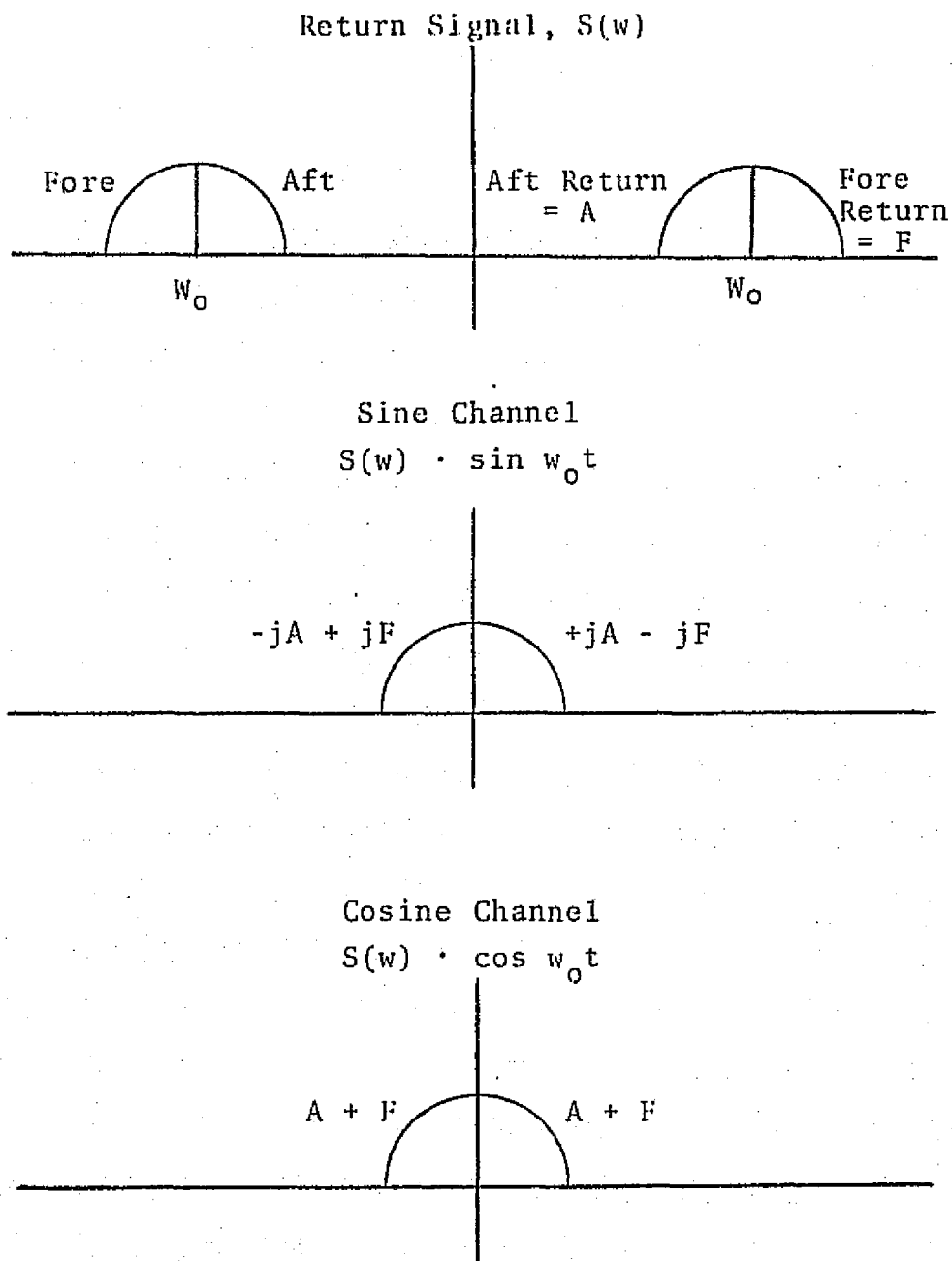


Figure 4. The NASA Scatterometer Output Signal

Spectrum Sampling and Cell Definition

The recovered spectrum, although usually centered around a lower and more convenient frequency, is otherwise identical to the original return spectrum. Each frequency corresponds to signal return from a unique angle of incidence. The return spectrum is sampled by a finite bandwidth filter which defines an area, or cell, on the ground. As shown by Jean [8], the sampled cell is outlined on the across track side by lines of constant Doppler shift having Doppler return frequencies equaling the upper and lower frequency limit of the band-pass sampled, while the along track sides are formed by the antenna beamwidth. The lines of constant frequency shift correspond to the intersection with the ground of cones of constant Doppler, concentric about the aircraft velocity vector.

In sampling the return spectrum, an estimate of the power return from a cell sampled is obtained. This estimate is then used in the determination of the scattering cross section. By plotting these lines of constant Doppler shift, called isodops, for a constant frequency difference, Δf , between each isodop, the cell definition and angular dependence can be demonstrated. Such a plot is given in Figure 5. The isodops are seen to form hyperbolas which for a constant Δf become more

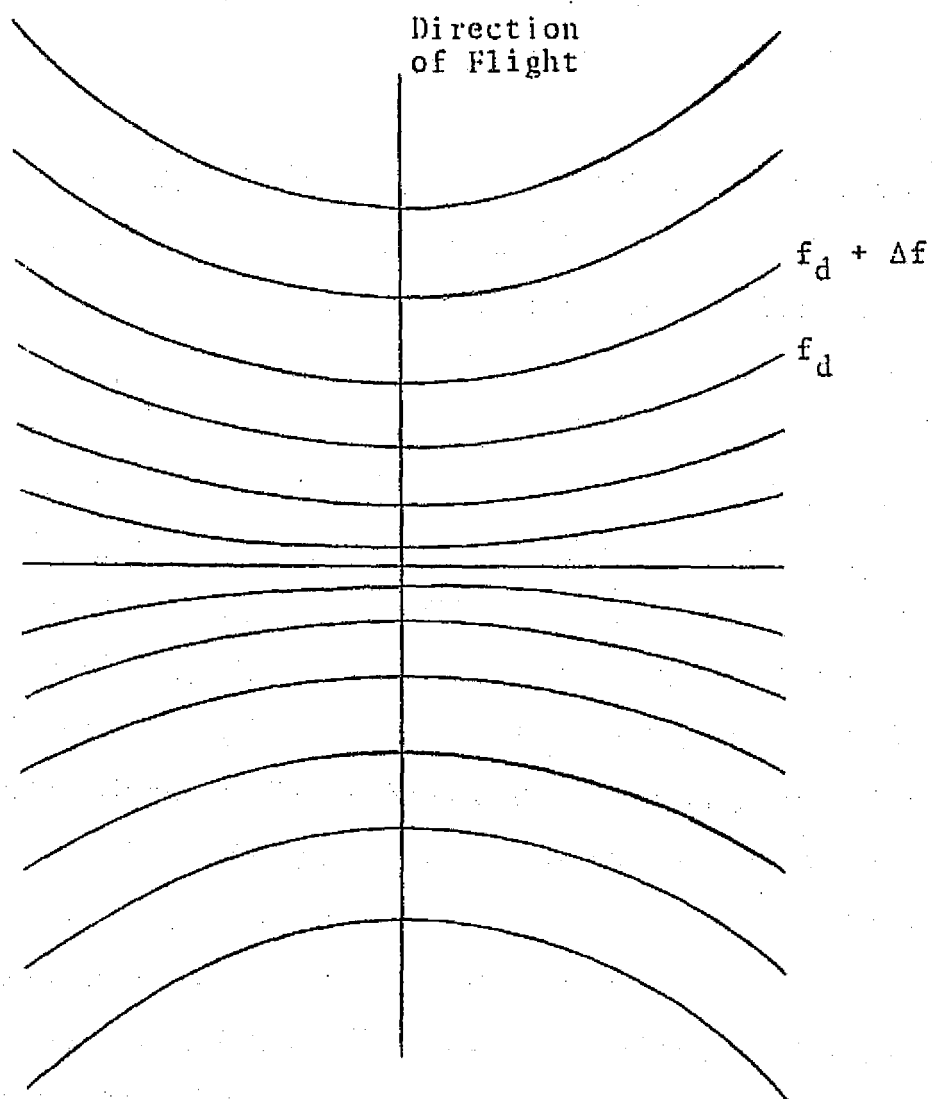


Figure 5. The Lines of Constant Doppler Frequency Shift, or Isodops.

widely separated as the angle of incidence increases. Thus, the cell length defined by the bandpass of the spectral sampling filter increases as the incident angle is increased. The cell area is then delineated by the intersection of the bandpass of the spectral filter and the limits imposed by the fan beam pattern of the antenna. A typical target cell is outlined in Figure 6.

When the aircraft roll or drift is introduced, the area within the antenna pattern changes. In Figure 7 is shown a typical target cell under aircraft roll or drift perturbations. The scattering cross section is calculated from this target cell.

Coefficient Calculation

The objective of scatterometer data reduction is to obtain the normalized scattering cross section, for a target cell, and ultimately to obtain a cross section function of a particular cell as a function of incident angle. Solution of the radar equation for σ° identifies the parameters which are needed for the calculation of cross section,

$$\sigma^\circ(\theta) = \frac{(4\pi)^3}{\lambda^2} \cdot \frac{1}{G^2(\theta)} \cdot \frac{R^4(\theta)}{A(\theta)} \cdot \frac{P_r(\theta)}{P_t}$$

The calculation of $\sigma^\circ(\theta)$ involves known constants, system parameters, calculated geometric parameters and dynamically

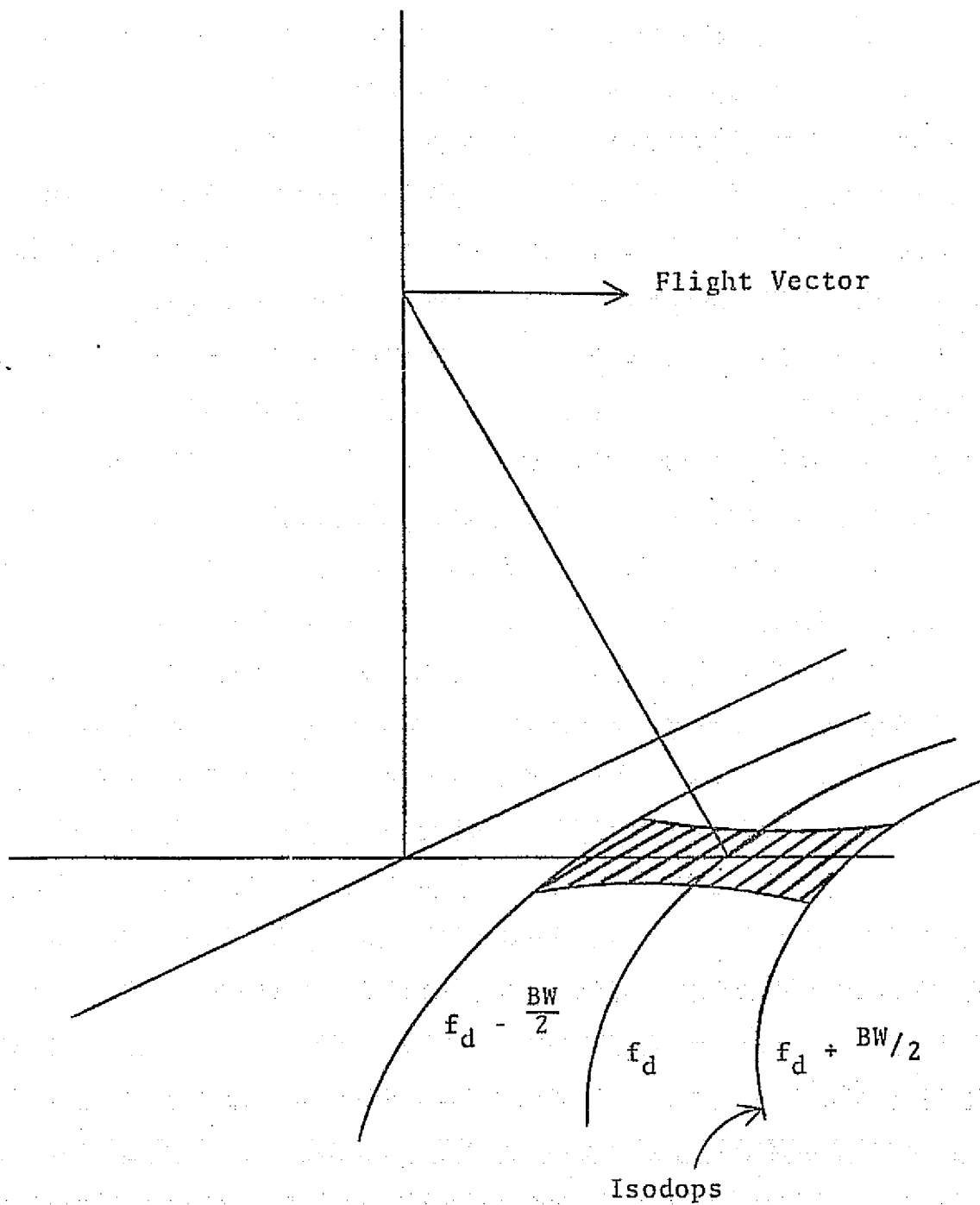


Figure 6. Instantaneous Ground Cell Area
with no Aircraft Perturbation

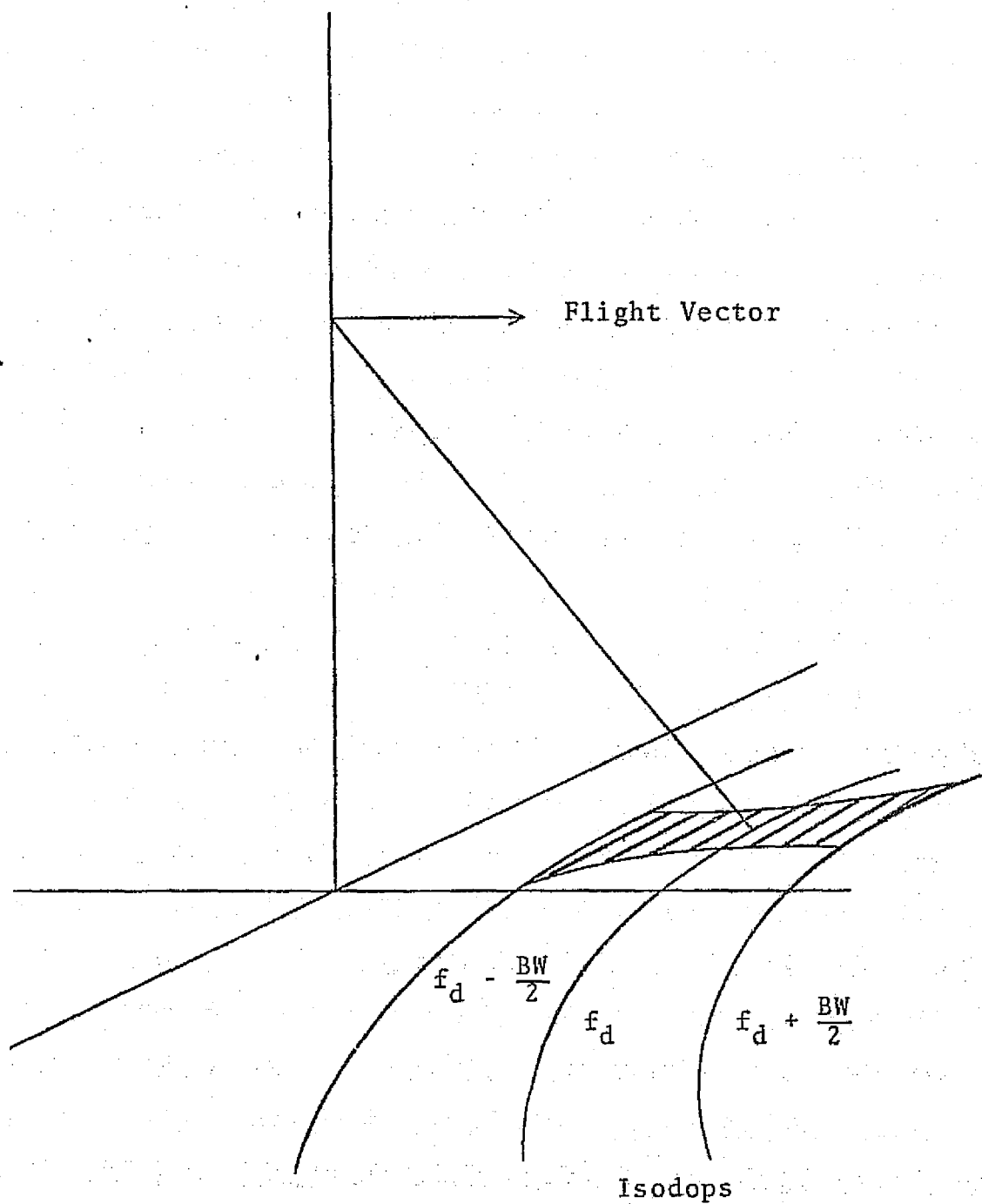


Figure 7. Instantaneous Ground Cell Area
with Aircraft Drift and/or Roll.

measured signal values. The system antenna gain parameter $G^2(\theta)$ is determined for the particular scatterometer system as a function of incident angle. The geometric parameters which appear in the solution of the radar equation are slant range to the target, R , and the illuminated cell area, A . These values are calculated using aircraft parameters which are dynamic rather than averaged values.

The processor determines both the transmitted and received power by measuring the sign-sensed radar signals through a bandpass filter. For a given angle, a Doppler frequency based upon aircraft parameters is calculated and the bandpass filter is set for that frequency. The output of the filter is related to the received power P_r . The filters are also set for the 12 KHz calibration voltage and its value is related to the transmitted power P_t . The ratio of powers required for the scattering coefficient calculation is obtained by

$$P_r(\theta)/P_t = \frac{H(f_\theta)E_\theta^2}{KE_{cal}^2}$$

where

E_{cal} = measured voltage for a filter frequency of
12 KHz

E_θ = measured output voltage

$H(f_0)$ = the frequency response characteristic
of the radar land/sea filter, and;

K = Ferrite Modulator Constant.

Alignment

The incident angle at which a target cell is viewed depends upon the relative position of the aircraft to that target. It is evident that the angle of incidence to a fixed target changes with the flight of the aircraft. Thus, radar return at different viewing angles from a single target cell must be measured at different times. Consequently, aligning the calculated scattering coefficients for a single target requires time shifting the calculated results. This time shift requirement is of major importance in providing a suitable data product from the scatterometer/processor system.

Processing Requirements

Thus, the processing requirements for the reduction of 13.3 GHz radar scatterometer data are identified.

The processor must:

- 1) sign-sense the signals to unfold the data into fore and aft spectra;
- 2) sample the power spectra at the appropriate frequencies to recover the radar return measurement and to obtain the measurement of the calibration level;

- 3) obtain the aircraft flight parameters so that geometric calculations of slant range and target area can be determined;
- 4) calculate the normalized radar cross section from the solution of the radar equation; and
- 5) time align the scattering coefficients from a single target so that the output from the processor gives aligned cross sections for each target area.

This set of requirements defines, in general, the functions which must be implemented by the processor to accomplish the required data reduction and presentation.

Functional Organization

In order to take advantage of the speed and efficiency of analog sign-sensing and spectral sampling, along with the accuracy and flexibility of digital computation, the RASP system combines both technologies to provide a hybrid system capable of real-time calculation of the scattering cross section. In Figure 8 is shown the functional organization of the RASP. The analog processor accomplishes the sign-sense and spectral filtering operations, while the digital processing section implements calculation, alignment and control functions. The digital processing section is developed around a microprocessor and, consequently, requires both hardware and software development.

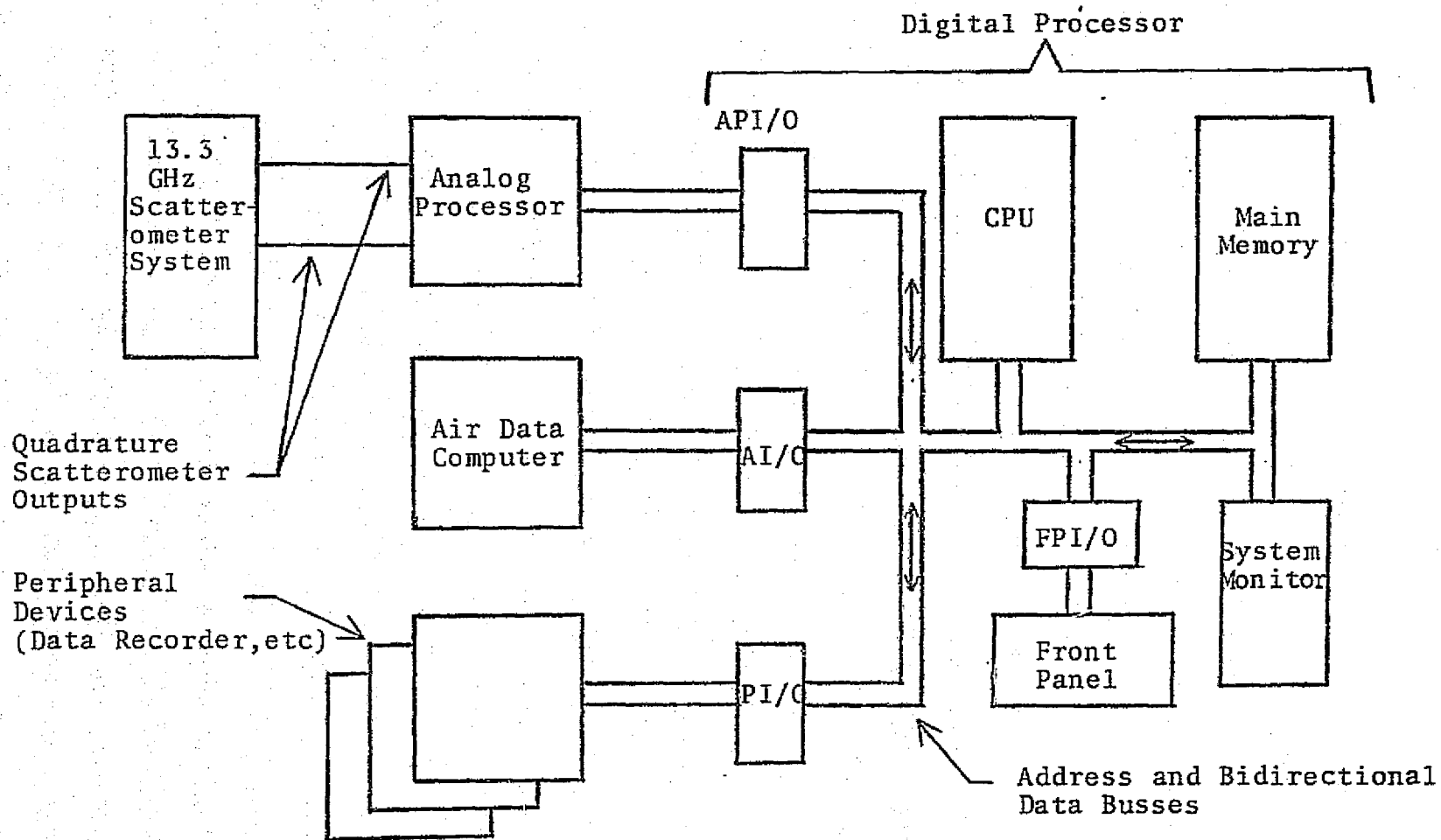


Figure 8. Block Diagram, RASP Processor

HARDWARE

The RASP system is designed to process signals generated by the NASA 13.3 GHz single polarized scatterometer. For real-time operation, it is necessary to accomplish the required processing functions by implementation of a hybrid analog-digital processor system. Signals provided by the scatterometer system are preprocessed, measured and converted to digital form by the analog subsystems. The digital subsystems implement a microprocessing environment which provides flexibility and precision in the computation of scattering cross sections. Additionally, the digital subsystem provides control for the selection of spectral sampling functions and digital conversion of signals at proper time intervals. The digital subsystems are developed to decode aircraft parameters available from a pcm stream and to provide processing results in a pcm stream compatible with NASA data reduction equipment. This section provides insight into the functional operation of the analog and digital subsystems. Additional detail is available in Processor Operation and Maintenance [9].

The Analog Subsystem

The analog processor subsection performs the sign-sensing and spectral sampling functions. Spectrum recovery is achieved by remodulating in quadrature the two baseband quadrature spectra output from the scatterometer

to a 20 KHz center frequency, then adding the two remodulated spectra. Figure 9 illustrates the total spectral separation procedure.

A detailed block diagram of the "sign-sense" and AGC circuitry is shown in Figure 10. Inputs 1 and 2 correspond to the sine (Redor 1) and cosine (Redop 2) channels of the scatterometer output. Unity gain buffer amplifiers provide the proper impedance termination for each channel.

The two quadrature data channels are filtered to remove out-of-band noise by amplitude and phase matched active filters. Following the filters the signals are again buffered, and an adjustment is provided to remove any DC offset voltage introduced by the filter circuitry.

The filtered sine and cosine channels are next mixed with separate 20 KHz signals which are themselves in phase quadrature. The resulting mixer outputs, both of which contain the folded fore and aft Doppler spectra centered at 20 KHz, are amplified and combined by sum and difference networks to yield the unfolded spectra.

An AGC signal is derived from the sum and difference channel outputs and is used to control the gain of the cosine channel such that the sine and cosine channels are maintained at equal amplitudes.

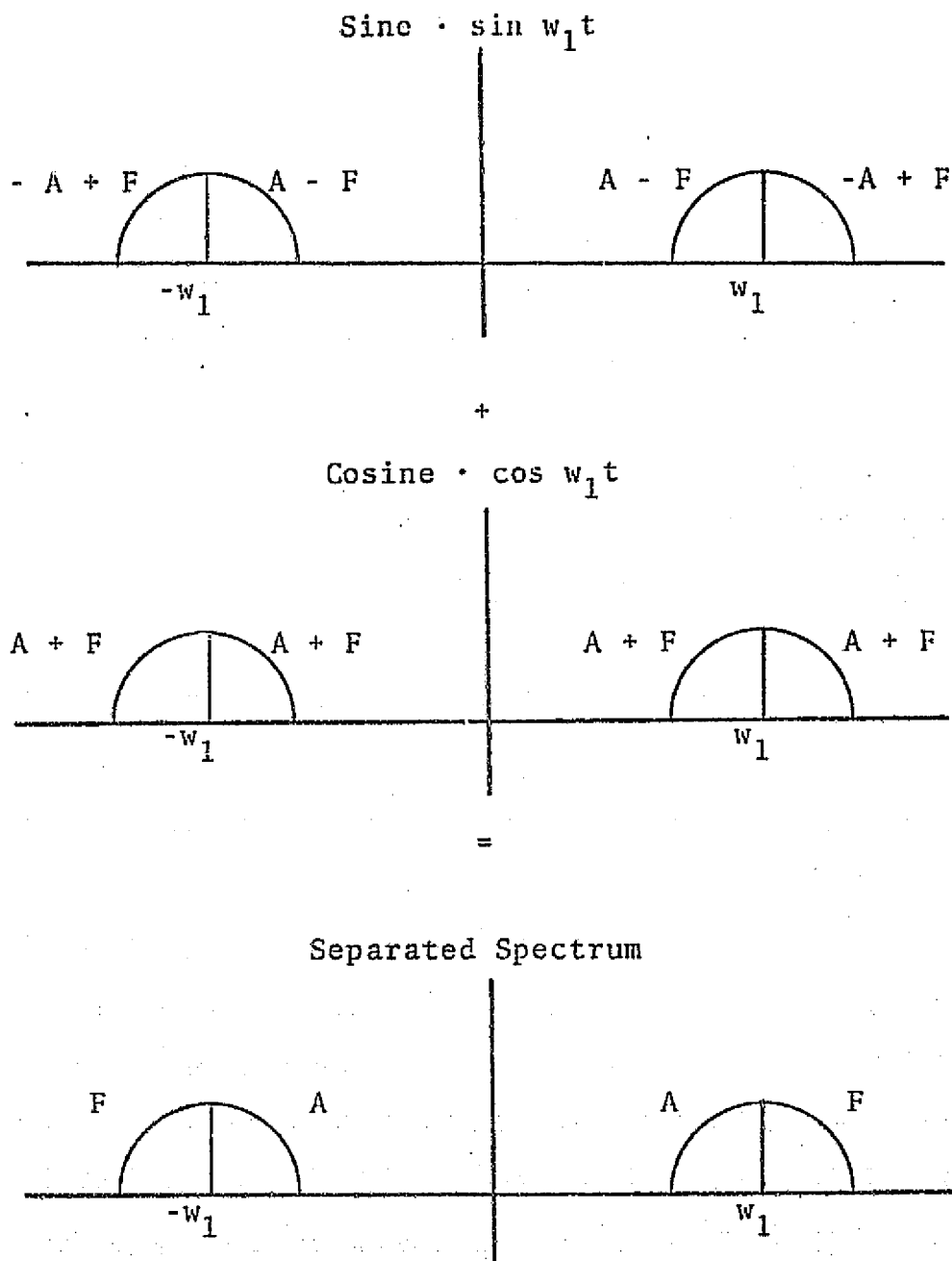


Figure 9. Doppler Spectrum Recovery

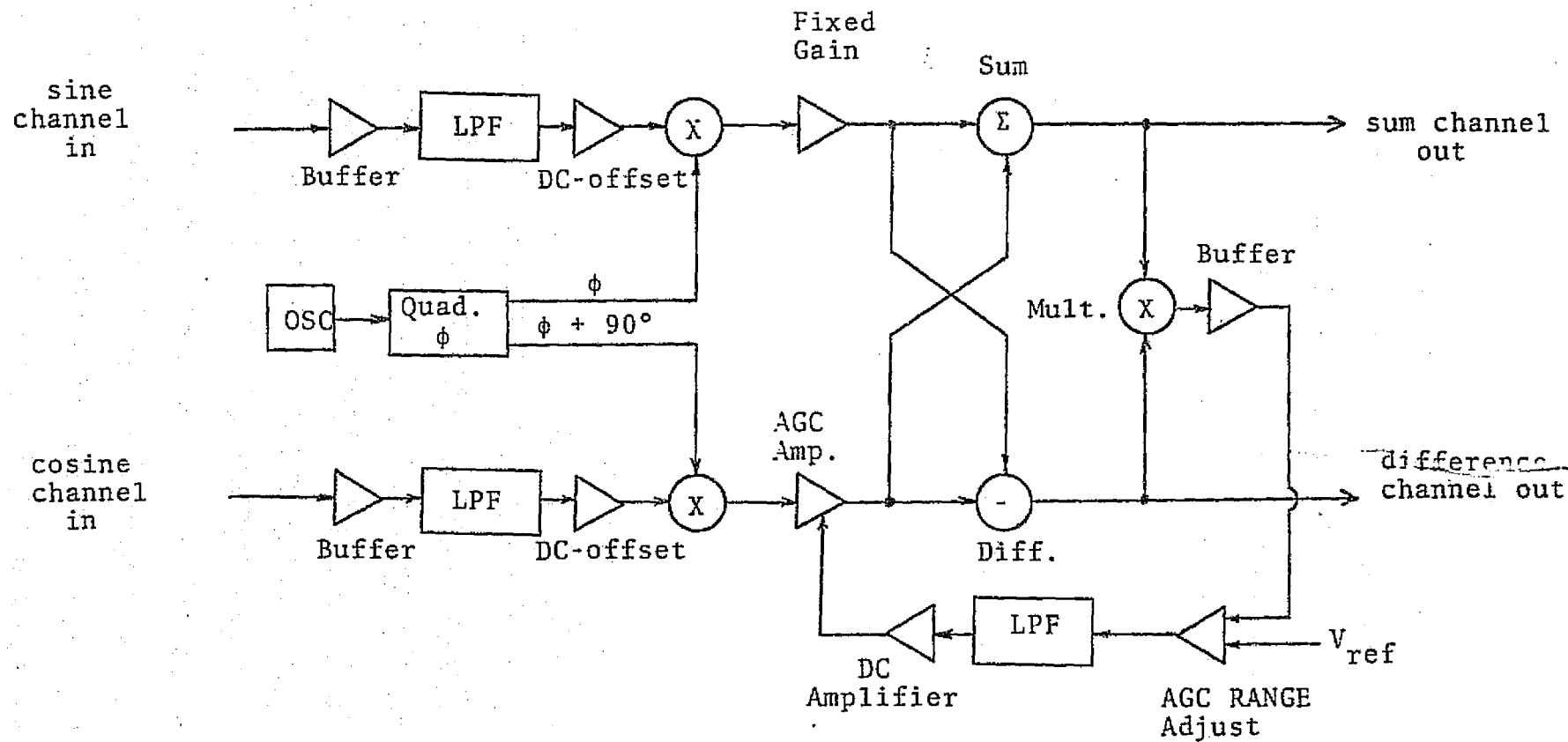


Figure 10. Block diagram of sign-sense and AGC sub-assembly.

The AGC voltage is produced by multiplying the sum and difference channels. This product yields a DC voltage proportional to the difference in the sine and cosine channel amplitudes plus higher frequency terms. This signal is filtered by a 20 Hz low-pass filter, amplified, and applied to the gain control input of the cosine channel post-mixer amplifier.

The spectral sampling subassembly consists of a voltage controlled oscillator (VCO), a balanced mixer, a 200 Hz low-pass filter, a linear integrator and an integrator as shown in Figure 11. In addition, there is a digital-to-analog converter which allows the digital processor to select the VCO frequency and an analog-to-digital converter which interfaces the output of the RMS module to the digital processor.

The digital processor calculates the required Doppler frequency corresponding to the particular angle to be sampled within a given sample interval. The processor outputs a digital word to the DAC to provide the correct DC tuning voltage to the VCO. The VCO output is applied to the balanced mixer, shifting the desired portion of the Doppler spectrum to zero center frequency. The mixer output is provided with a DC offset adjustment to zero the DC output level for zero input signal. This output is then filtered by the 200 Hz low-pass filter.

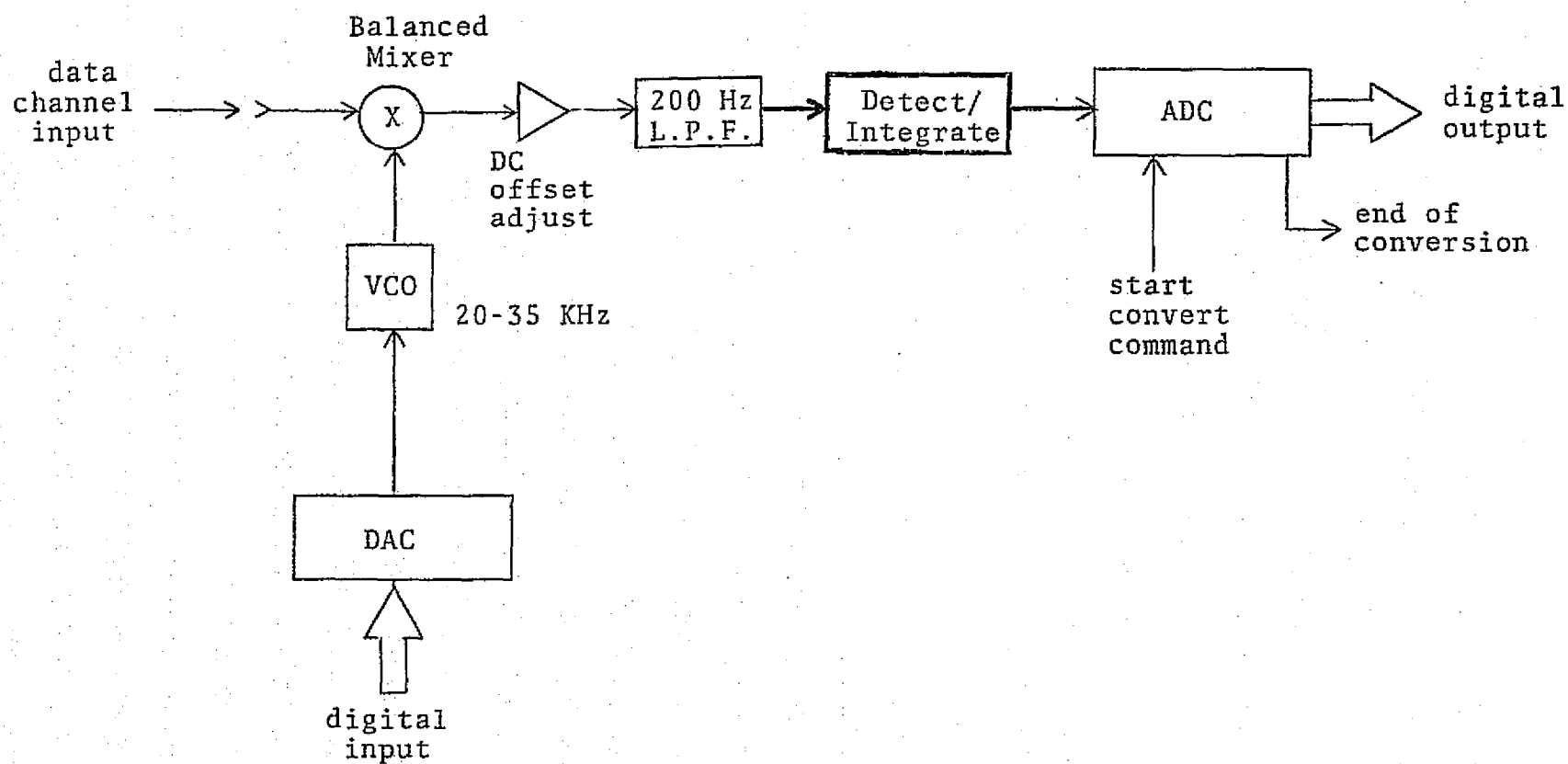


Figure 11. Block diagram of spectral sampling and digital interface subassembly.

The filter output, which is that portion of the processed signal from the desired Doppler resolution cell, is applied to the input of the linear detection and the output is integrated.

After an integration period of 0.1 second, the signal is sampled by the ADC on command from the digital processor. The output of the ADC is a digital word which is proportional to the RMS voltage of the 200 Hz filter output. The square of this voltage is therefore proportional to the power received from the target within the Doppler resolution cell.

The Digital Subsystem

The primary function of the digital section of the RASP is the calculation of σ^0 from the radar equation. This calculation, including computation of the cell area and range, is carried out in the Central Processing Unit (CPU). The CPU, actually a small digital computer, also provides control of the analog system in selecting the frequency setting of the VCO for sampling angle determination and control of peripherals for data transfer such as a data recording device.

Computer systems studied in the selection of the central processor ranged from minicomputers to microprocessors. Evaluation of the systems by Cariker [8] shows

that minicomputers are actually more powerful than required and that the most desirable choice would be a microprocessor-based CPU. Recent advances in integrated circuit technology have made possible these single chip processors with inherently high reliability and economy. A study of the available microprocessors, with consideration of such factors as speed, computational power, availability, reliability, software and hardware support and simplicity of design, led to the choice of the Intel 8080 8-bit microprocessor as the base of the central processing unit.

The Intel 8080 is an 8-bit central processing unit chip which has the capability of addressing up to 64 K bytes of memory and up to 256 external devices. The 8080 has a machine cycle execution time of 500 nanoseconds with three to five cycles required per instruction.

The digital subsystem is developed on a bi-directional bus structure. Control lines are available to each device on the bus so that the CPU function can be affected by peripheral units. The CPU controls peripheral units by way of an address bus and by certain control lines which indicate whether a read or write operation is being initiated.

Various interface units to the CPU provide access to the data needed for the calculations. The analog subsystem functions as a peripheral to the CPU

with separate ports provided for the setup of the analog spectral filter center frequency and for the reading of the converted digital signals obtained from the analog-to-digital conversion unit.

A separate digital controller and CPU peripheral accepts the aircraft state parameter from a serial digital data stream. The aircraft interface controller is capable of accepting either NERDAS or ADAS digital data. The aircraft interface continually updates its internal buffer memory with newly acquired data. During certain idle portions of the controller cycle, the buffer memory is available to the CPU to transfer the latest available aircraft parameters. Upon CPU initiated reads, the information is transferred to memory.

There are several output modes for the processor system. Two serial digital interfaces are implemented to provide for data output. These include a standard communications interface which is compatible with Electronics Industry Associates (EIA) specification RS-232/C. This interface is secondary to the Bi-phase Level (Bi-ØL) output used operationally. This particular format is compatible with NASA data acquisition systems so that processor output can be recorded under flight conditions and subsequently reduced and tabulated with standard reduction equipment and procedures. Analog outputs are

also provided for strip chart recording of processed scattering coefficients.

Operator communication and programming is provided by front panel functions. The front panel is divided into two sets of switches for operator interaction. The top set of switches are primarily for system programming and diagnostic testing. These switches are normally unavailable to an operator during operational flight conditions. The lower half of the front panel is the operator's console. These switch functions and displays provide the operator with a procedure for defining a particular processing configuration. The displays provide some monitor capability and warning lamps indicate failure of various parts of the subsystem. Operation modes are also controlled by an operation from the front panel.

SOFTWARE

Processor software is implemented to provide control, computation and testing functions for the RASP. Various programmed modes are available and operator selection of these modes controls the processor functions. Computational sequences and data acquisition parameters are controlled by the processor software and preprocessed radar signals are converted to normalized scattering cross sections through software controlled calculations. Floating point arithmetic is accomplished through the software package. Comprehensive diagnostic procedures are software controlled to assume proper operation of the RASP system.

Modes

The processor software operates in several basic modes according to operator selection. These modes of operation include Internal Calibration, Self-Test, Idle, Run, Halt and Reset. A flowchart involving these modes with brief descriptions is shown in Figure 12. The principal modes of interest are Idle, Self-Test and Run. The Reset mode allows the operator to reset the processor operation to a specific program initiation point. This reset is manually activated and can be accomplished during any phase of the processing. The Self-Test mode provides for a software guided procedure to test major hardware functions related to operator interface, memory malfunction,

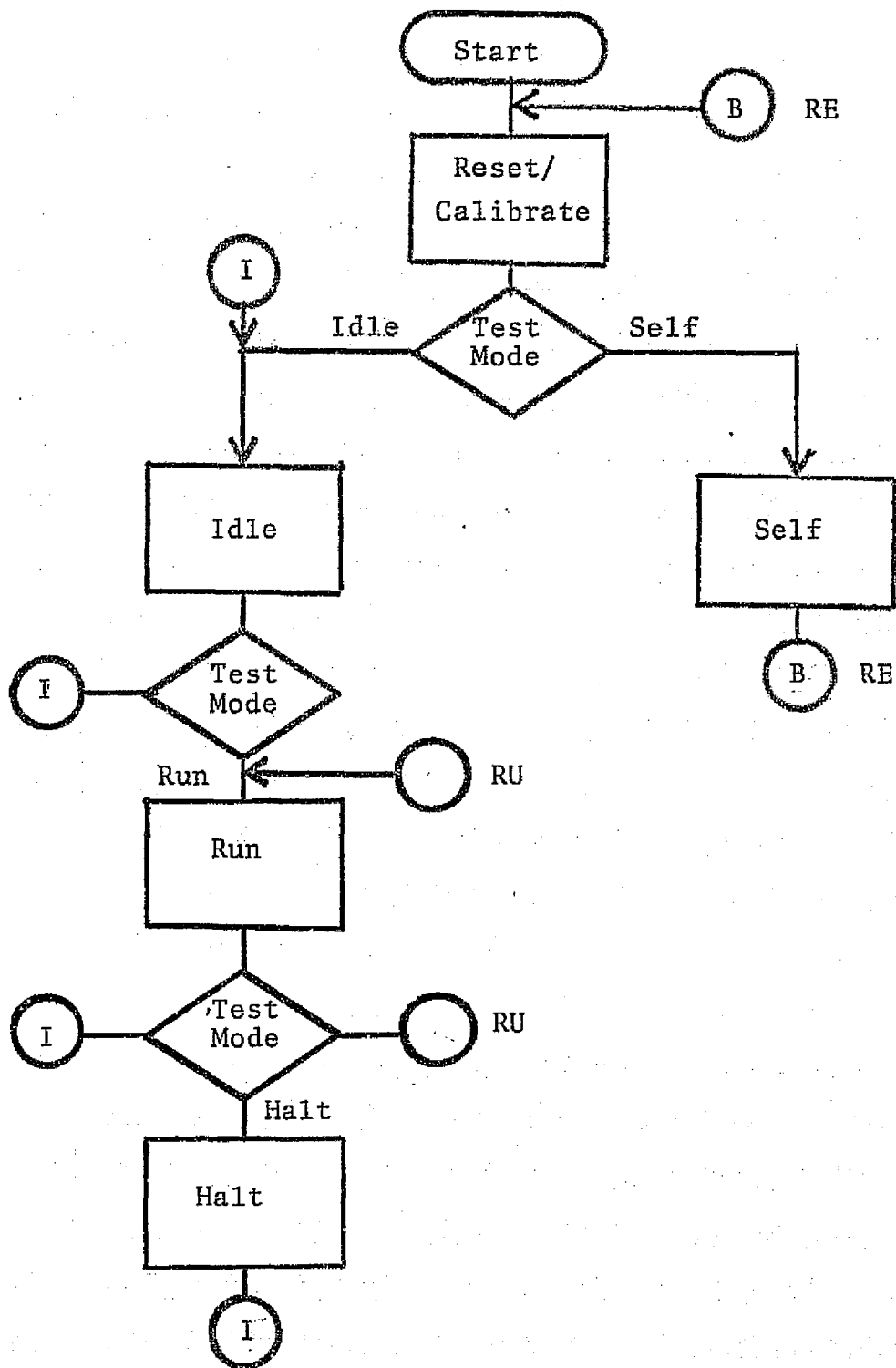


Figure 12. Flowchart of Processor Modes

analog sign-sense, strip chart output and scatterometer calibration signal acquisition. The procedures for operation of the Self-Test software are provided in Processor Operation and Maintenance [9].

In the Idle mode, the operator defines the configuration setup for the processing to be accomplished. Angle selection, fore-aft target selection, and input and output channels are selected. This mode also allows for operator definition of aircraft flight parameters to be used for processing. Once a correct processing configuration is determined, the operator can initiate the Run mode for processing of data.

When the Run mode is selected, the processing of radar signals is initiated. The Run mode activates an acquisition cycle which is composed of a calibration step and ten coefficient calculation steps. Each step is accomplished in 100 ms; consequently, the acquisition cycle is 1.1 seconds in duration. During the calibration step, the filtered voltage corresponding to the scatterometer calibration signal at 12 KHz is measured. It is this value which is used for scattering coefficient calculation during the remaining cycle steps. It is also during this step that the bandpass filter is set up for viewing the signals at the next angle to be processed; the frequency of the filter for the next angle to be measured is calculated;

the aircraft flight parameters for the calculation steps are determined; and the data obtained for the completed target cell are output. During the calculation phase of this step, signals are being filtered and integrated for the next angle to be processed.

The coefficient calculation steps are identical except for the actual angle selected. The calculation step begins by sampling and analog-to-digital conversion of the filtered and integrated signals to be used in the scattering coefficient calculation. The integration time is fixed at 100 ms and the software waits until the integration is complete before the measurement is made. Once the signal is measured, the bandpass window of the processor is changed and integration at the next angle is initiated. While this integration is being accomplished, the data last acquired are processed. During this time, the frequency for the next angle to be filtered is determined; the measurement is converted to floating point; the power ratio is computed; target cell area is computed using aircraft flight parameters; the scattering coefficient is calculated; the coefficient is converted to decibels; and the data value is stored in an accumulation array for alignment. The step is thus completed and another calculation step is initiated until a total of ten calculation steps are taken.

In the tenth calculation step, the bandpass filter is set up to view the scatterometer calibration signal and upon the completion of this step, the calibrate step is initiated.

The Run mode is active until an operator selects either Halt, Idle or Reset, at which time the Run mode terminates and the selected mode is initiated. The Halt mode provides for an orderly termination of processing steps where the Reset mode causes immediate termination. In the present implementation, there is little difference between terminating through the Halt mode or terminating directly into the Idle mode.

A typical operator sequence involves turning the processor on and allowing a suitable warmup time. The next step is to select the Self-Test mode and to Reset the system. At this point, the Self-Test procedure is followed to assure that the processor is functional. Upon successful completion of the Self-Test procedure, the processor initiates the Idle mode. An operator selects the appropriate flight/processing configuration at this time and observes the processor confirmation of a correct setup. The next step is to initiate the Run mode at the beginning of the flight line. As the measurement line is completed, either Halt or Idle is selected to terminate the processing operation. With

the processor in the Idle mode, the configuration can be modified to accommodate changes for the next flight line.

Arithmetic

The processor software is required to perform arithmetic and transcendental function over a broad range of numerical values. Calculation of the composite equation for the scattering coefficient requires numerous multiplies and divides. It also requires additions and subtractions but to a lesser degree. Floating point arithmetic is implemented for the processor due to the large dynamic range of the calculations. Since a larger number of multiplies and divides are required, the floating point representation is in a logarithmic form. Multiplication is accomplished simply by the addition of logarithms.

Sixteen bits are used to represent floating point numbers. In the logarithmic form, the most significant bit of the number is the sign bit. When this bit is on, the number is negative. The next most significant seven bits are the characteristic of the logarithm in two's complement representation and the least significant eight bits represent the mantissa as an unsigned fraction with the binary point immediately preceding it. The base of the logarithm is two.

A second form for floating point is used for the addition and subtraction of numbers. For the most

part, this form exists only internal to the addition and subtraction routines. This form is described here for completeness. The non-logarithmic form is similar to standard scientific notation where a number is represented by a fraction and a power of the radix. In this representation, the 16-bit binary number has the most significant as a sign, the next most significant seven bits are the power of the radix two and the eight least significant bits are the binary fraction with the binary point assumed to precede them. The two representations are shown in Figure 13.

Multiplication using logarithms is based on the relationship;

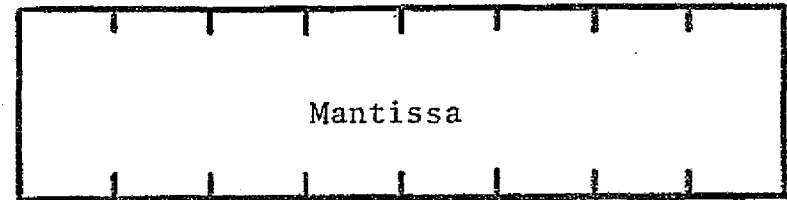
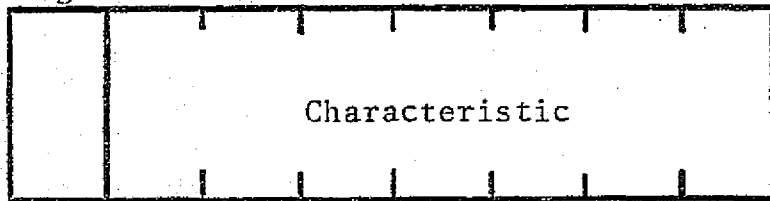
$$\log AB = \log A + \log B$$

and division is accomplished by

$$\log A/B = \log A - \log B$$

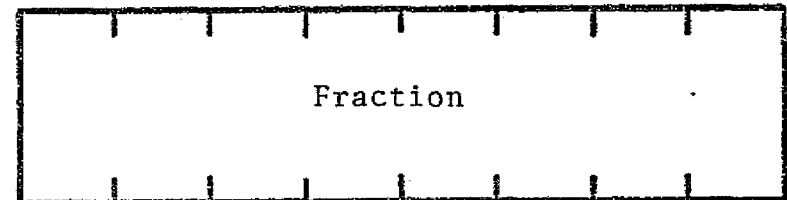
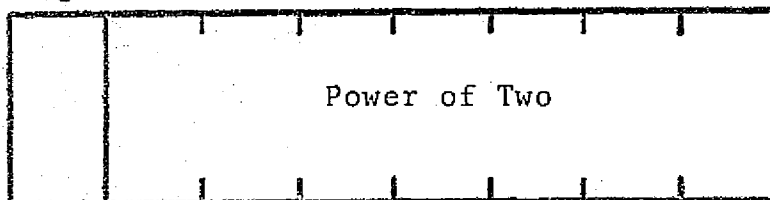
Multiplication is performed by binary addition of the logarithms of the floating point numbers which produces logarithms of the product. Likewise, division is determined by finding the binary difference. Since the normal representation of the numbers is in a logarithmic form, multiplication and division software merely provides for the binary addition and subtraction. Results which would produce characteristics outside the maximum range of from +63 to -64 are set to the extreme value. The logarithmic

Sign



Log Format

Sign



Floating Point Format

PROCESSOR NUMBER REPRESENTATION

Figure 13.

representation of zero is the smallest possible value, that is a logarithm with a characteristic of -64. Arithmetic functions and conversion tables return this value for zero when appropriate.

It is noted that addition and subtraction are performed as true floating point numbers. Consequently, the number must be converted from the logarithmic form for the additions to be performed and returned to the logarithmic form for internal program consistency. The conversion between the two forms is accomplished by a table look-up procedure. The mantissa and binary fraction of the two forms are converted by the table and the characteristic and power-of-two are determined by the relationship,

$$\text{Power-of-two} = \text{characteristic} + 1.$$

Once the numbers are converted from logarithmic form, the fraction must be aligned according to the power-of-two. The smaller fraction must be logically shifted right and the power-of-two of the number incremented until the powers of both operands are equal. If the signs of the operands are different, the fraction of the negative operand must be complemented before addition. If the result of the operation is non-zero, and the most significant bit of the fraction of the result is not set, then,

post normalization is necessary. This is accomplished by shifting the fraction of an operand left and by decrementing the power-of-two until a one appears in the most significant bit position of the fraction. At the end of the addition/subtraction routine the answer is converted to logarithmic form.

Functions like sine, cosine and tangent are look-up functions where the input argument is expressed either in degrees or tenths of degrees in an 8-bit unsigned integer representation and the appropriate function routine is called. The entry corresponding to the value of the desired function is retrieved. A square root function is implemented which divides the logarithm of the floating point number by two. The routine returns a logarithmic zero for operands less than zero.

The subroutines for the floating point arithmetic operations were initially written in Texas Instruments 980A assembly language. Since the 980A supports FORTRAN, a test program was written to compare the results of the microprocessor simulation with known reliable results. Once the results from the two software packages agreed, the floating point software was converted to the microprocessor assembly language, retested, and integrated into the processing software.

Area Calculation

A critical parameter in the calculation of scattering cross section is the area of the target resolution cell viewed by the radar system. As previously discussed, the target cell is limited by the Doppler contours corresponding to the bandpass edges of the spectral sampling filter and by the limits imposed by the antenna pattern. These cell boundaries change as a function of aircraft altitude and velocity as well as aircraft attitude parameters of roll and drift. Pitch does not affect the area definition.

The most exact method for calculating the target area is to perform a numerical integration over the cell boundaries; however, this is unreasonable in light of real-time processing constraints. When certain approximations are applied to the problem, a closed-form solution for calculation of area is obtained. An approximate area is determined by obtaining the width of the terrain cell at the nominal look angle, as determined by the beamwidth of the antenna pattern, and multiplying this by the length of the cell as determined by the intersection of the Doppler contours associated with the band edges of the spectral sampling filter. Equations for each of these curves are developed in [8] and the resulting area term is defined as

$$A = \frac{w'(y_2 - y_1)}{\cos \theta}$$

where

$$w' = \frac{2h \tan B/2}{\cos \cos}$$

$$y_i = \frac{h \cos \phi}{1 - K_i \cos^2 \phi} \left| \tan \phi \tan \psi \pm \sqrt{\tan^2 \psi (K_i - 1) + K_i \cos^2 \phi - 1} \right|$$

$$k_i = \left(\frac{2V}{f_i \lambda} \right)^2 \quad i = 1, 2$$

$$f_1 = f_d - \frac{\Delta f}{2}$$

$$f_2 = f_d + \frac{\Delta f}{2}$$

and

$$f_d = \frac{2V \sin \theta \cos(\alpha + \phi)}{\lambda}$$

In these equations,

h = aircraft altitude

v = aircraft velocity

θ = look angle measured from aircraft nadir

ϕ = aircraft drift

ψ = aircraft roll

β = antenna across track beamwidth

$\alpha = \sin^{-1} (\tan \psi / \tan \phi)$

Δf = bandwidth of spectrum sampling filter

λ = wavelength of transmitted energy.

Coefficient Alignment Procedure

Alignment of the scattering coefficients from a single target is a major processor requirement. A processing algorithm has been developed which makes the alignment of computed coefficients a straightforward procedure. The cycle time required for the sampling of signals from all of the viewing angles defines the time between target cells which have been processed. The number of major cycles to be completed before a cell is overflowed provides a convenient cell index. This index is used as the pointer to an array in which the values of the scattering coefficients and certain aircraft parameters are stored which relate to the indexed target cell. Cell alignment is accomplished by saving a computed scattering coefficient in the appropriate array position and reading out all the coefficients and aircraft parameters for a specific cell when all of its data have been acquired.

In Figure 14 is shown a diagram of the cell acquisition sequence. Each ground cell is referenced by a sequence number which is the pointer into the array where values associated with that target cell are saved. This array is shown in Figure 15. Note that all of the scattering coefficient values for the fore angles $(\sigma_0^\circ - \sigma_3^\circ)$ have been acquired for the i th target cell.

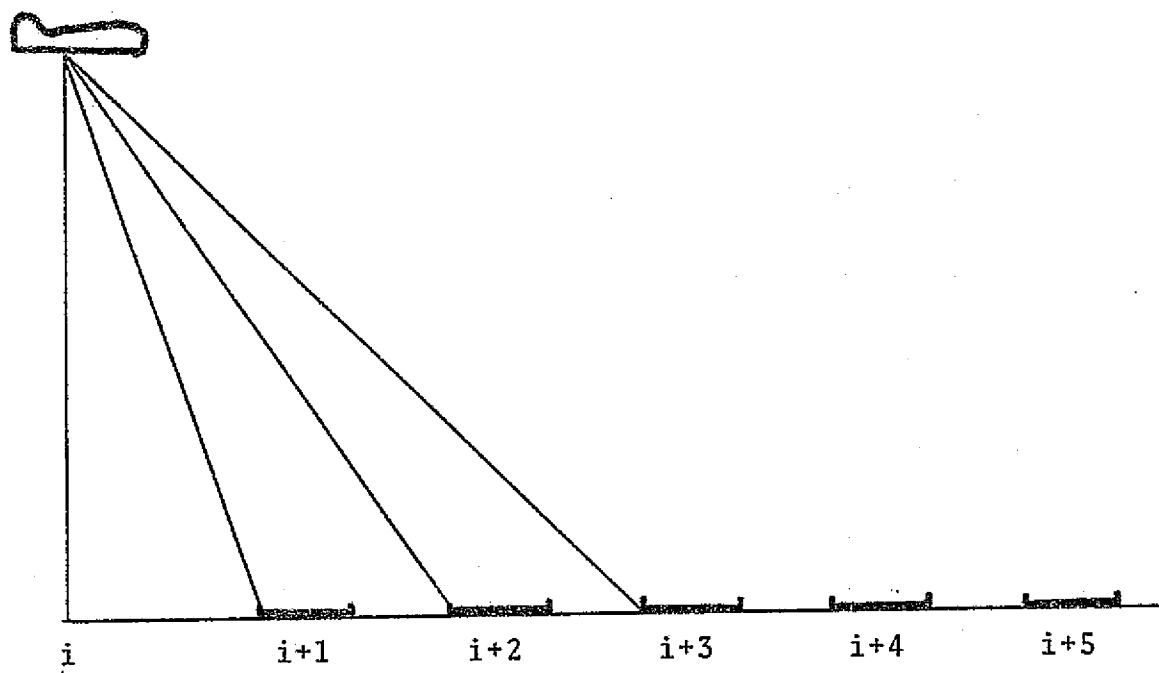


Figure 14. Cell Acquisition Sequence

000					
i	σ_0°	σ_1°	σ_2°	σ_3°	000
i+1		σ_1°	σ_2°	σ_3°	000
i+2			σ_2°	σ_3°	000
i+3				σ_3°	000
i+4					000
000					

Figure 15. Coefficient Alignment Array

During the next acquisition cycle, the aircraft advances along the ground track by one target cell, and the index i is increased by one. In other words, the nadir point of the aircraft is at cell $i + 1$. The radar acquires cell $i + 4$ at the largest angle and σ_3° for the $i + 4$ th cell is computed. Similarly, for the $i + 3$ rd target cell, σ_2° is computed, for the $i + 2$ nd target, σ_1° is computed, and σ_0° for the $i + 1$ st cell is computed. These coefficient values are saved in the alignment array corresponding with the index of the target cell and the particular angle associated with the coefficient. The array thus fills with each new acquisition and as the aircraft overflies the ground cell, associated flight parameters are also saved.

At the time of overflight, all the information about the target cell has been acquired for the forward look direction. If this is the total information required, then the aligned scattering coefficients for this target cell can be output along with the associated flight parameters at that point in time. Should the array position be continually reserved for a single cell, then as additional cells are acquired, the array size grows without bound. However, after the data are output, there is no further need to save their position in the alignment array.

Modulo arithmetic is implemented in the alignment algorithm for the index pointer into the array. If the array is of a fixed size large enough to accommodate all target cells which are viewed by the radar at a single instant, and the pointer to the array is computed modulo that number or larger, then as a data set is output for a particular target cell, this array position is assigned to a newly acquired target cell. In this manner the array is of a fixed and, thus, bounded size, and an efficient utilization of storage memory is accomplished.

The accommodation of aft data is a simple extension of the procedure outlined and requires an array which is twice as large. The minimum size of the accumulation array for fore and aft data is given by the formula

$$N = \frac{2h \tan 60^\circ}{vT}$$

where

N = the number of indexed vectors

h = aircraft altitude in meters

v = aircraft velocity in meters/second; and

T = length of the acquisition cycle (sec).

For a fixed array size, the value of N is fixed and, consequently, each set of flight parameters must be checked to see if the array size is exceeded. The implemented

software checks this bound and if it is exceeded, defaults to a condition where the data are output as acquired without further alignment.

Scattering coefficients which have an angle causing them to fall between the discrete target cell positions are assigned to the nearest target cell. Consequently, the average misalignment of scattering coefficients is not greater than half the target cell separation distance. In Figure 16 is shown a graph of permissible values of v and h for the specific software installation delivered with the processor.

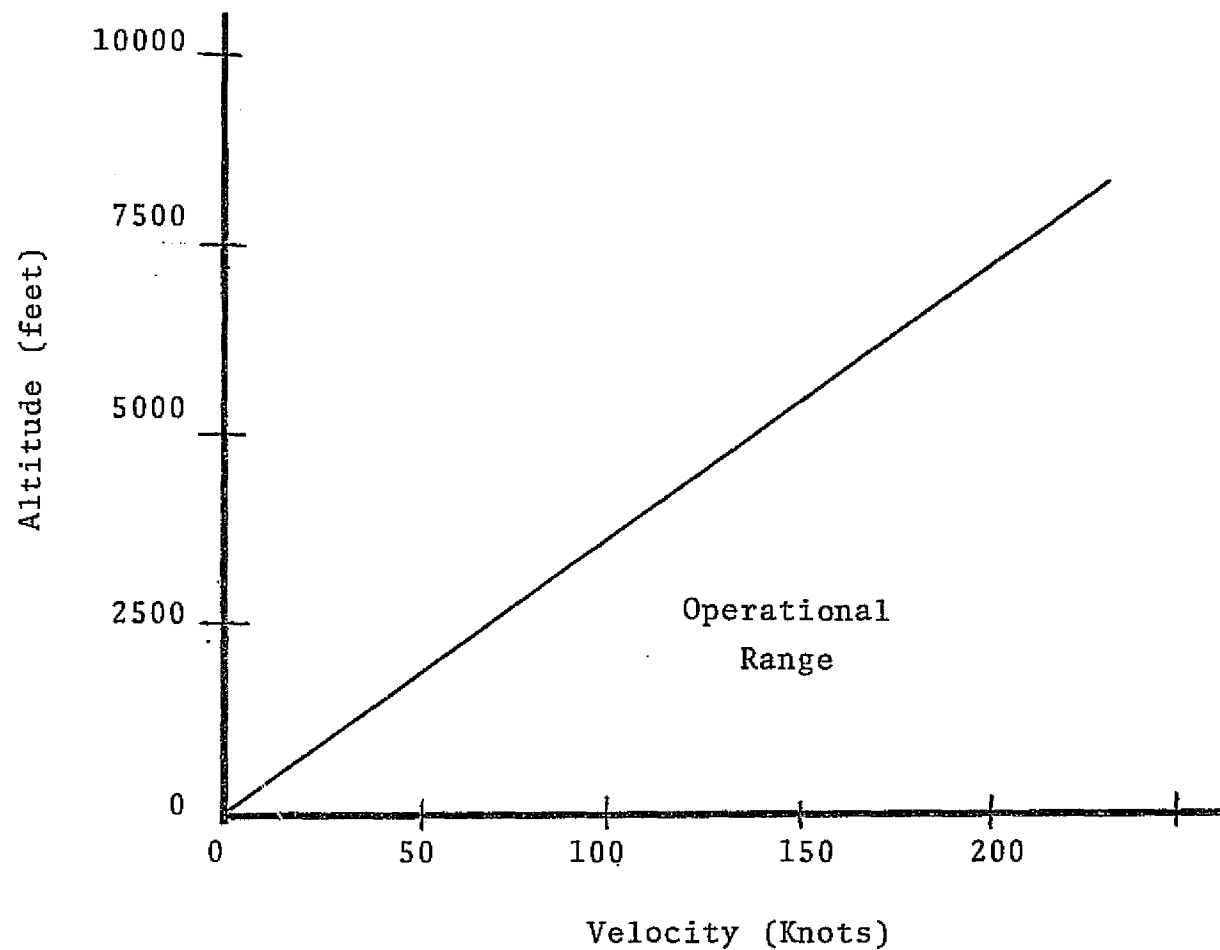


Figure 16. Aircraft Operational Range for Coefficient Alignment

CONCLUSIONS AND RECOMMENDATIONS

A Real-Time Airborne Scatterometer Data Processor (RASP) has been developed to provide for reduction of the signals from the NASA 13.3 GHz, single polarized radar scatterometer system. This processor unit has extended previous techniques for the real-time hardware processing of scatterometer data. Previous development stopped short of actual scattering coefficient calculation. This development has provided for that calculation showing methods and procedures for its implementation. The unit has been developed beyond a feasibility demonstration model and actually provides for engineering evaluation of the processing techniques under limited flight conditions. Design goals for the system have been exceeded and the final unit provides improved flexibility, precision and data format.

Other conclusions can be made. A design goal of 100 ms steps in signal measurement and the calculation of the scattering cross section has proven to be a conservative number. It is estimated that an approximate 15-20 percent improvement in the time performance of the processor algorithms could be met primarily by shortening the per point integration time. This improvement would result in the availability of closer target cells.

Observations of the total system have identified some problem areas. An unbalanced 60 Hz noise exists on one channel of the radar system. This signal is at times large enough to drive recorders into saturation for high noise peaks. Additionally, the existence of this noise on one channel and not on the second channel tends to defeat the AGC design implemented in the processor. Additionally, it has been observed that the VCO in the spectral sampling circuit is not as stable as would be desired. The resolution of the processor is reduced to make up for this uncertainty.

Since this unit was involved in a development, it is more flexible than would be required for a strictly operational system. It is recommended that should similar processors be developed, their complexity be reduced from that of the current processor system. The programmer panel functions would more appropriately be placed into a test set rather than on the front panel. It seems reasonable that additional self-test steps could be added to facilitate processor alignment and repair. Specifically, steps to set upper and lower limits for the VCO would be useful.

Determination of the radar calibration level through an alternate means offers some advantages concerned with VCO drift and some disadvantages regarding common

channel gains. It is recommended that alternate methods for the extraction of calibration signals be investigated for further developments of this variety. If unbalanced noise continues to exist in the 13.3 GHz scatterometer system, it is recommended that consideration be given to the disabling of the processor AGC provided channel gains can be maintained at like values.

In future systems, additional consideration should be given to implementation with microprocessor circuits other than the Intel design. It is felt that the state-of-the-art in this area is changing at such a rate as to make current evaluation of products obsolete in a short time. Although the Intel system is most viable at this time, changes in technology may change this position.

REFERENCES

- [1] B.R. Jean, "Radar Studies of Arctic Ice and Development of a Real Time Arctic Ice Type Identification System," Final Report 3005-6, Remote Sensing Center, Texas A&M University, January 1976.
- [2] R.G. Reeves, Editor-in-Chief, Manual of Remote Sensing, American Society of Photogrammetry, 1975.
- [3] M.I. Skolnik, Ed., Radar Handbook, McGraw-Hill Book Company, 1970.
- [4] M.W. Long, Radar Reflectivity of Land and Sea, Lexington Books, 1975.
- [5] T.F. Bush and F.T. Ulaby, "Radar Return from a Continuous Vegetation Canopy," IEEE Transactions on Antennas and Propagation, Vol. AP-24, pp. 269-275.
- [6] J.W. Rouse, Jr., H.C. MacDonald and W.P. Waite, "Geoscience Applications of Radar Sensors," IEEE Transactions on Geoscience Electronics, Vol. GE-7, January 1969, pp. 2-19.
- [7] G.A. Bradley, "Remote Sensing of Ocean Winds Using a Radar Scatterometer," Remote Sensing Laboratory Technical Report 177-22, September 1971.
- [8] J.A. Schell et al., "An Airborne Radar Scatterometer Signal Processing System," Progress Report RSC 3182-1, Remote Sensing Center, Texas A&M University, May 1975.
- [9] J.A. Schell et al., "Processor Operation and Maintenance," Report RSC 3182-2, Remote Sensing Center, Texas A&M University, December 1976.